Dossier

This paper is a part of the hereunder thematic dossier published in OGST Journal, Vol. 70, No. 1, pp. 3-211 and available online here

Cet article fait partie du dossier thématique ci-dessous publié dans la revue OGST, Vol. 70, n°1, pp. 3-211 et téléchargeable ici

DOSSIER Edited by/Sous la direction de : **B. Leduc et P. Tona**

IFP Energies nouvelles International Conference / Les Rencontres Scientifiques d'IFP Energies nouvelles
E-COSM'12 — IFAC Workshop on Engine and Powertrain Control, Simulation and Modeling
E-COSM'12 — Séminaire de l'IFAC sur le contrôle, la simulation et la modélisation des moteurs et groupes moto-propulseurs

Oil & Gas Science and Technology – Rev. IFP Energies nouvelles, Vol. 70 (2015), No. 1, pp. 3-211

IFP Energies nouvelles

Oil & Gas Science and Technology – Rev. IFP Energies nouvelles, Vol. 70 (2015), No. 1, pp. 143-158

DOI: 10.2516/ogst/2013210

IFP Energies nouvelles International Conference
Rencontres Scientifiques d'IFP Energies nouvelles

E-COSM'12 - IFAC Workshop on Engine and Powertrain Control, Simulation and Modeling
E-COSM'12 - Séminaire de l'IFAC sur le contrôle, la simulation et la modélisation des moteurs et groupes moto-propulseurs

Integrated Energy and Emission Management for Diesel Engines with Waste Heat Recovery Using Dynamic Models

Frank Willems[1,2*], Frank Kupper[2], George Rascanu[1] and Emanuel Feru[1]

[1] *Eindhoven University of Technology, Faculty of Mechanical Engineering, P.O. Box 513, 5600 MB Eindhoven - The Netherlands*
[2] *TNO Automotive, Steenovenweg 1, 5708 HN Helmond - The Netherlands*
e-mail: f.p.t.willems@tue.nl - frank.kupper@tno.nl - g.c.rascanu@student.tue.nl - e.feru@tue.nl

* Corresponding author

Abstract — *Rankine-cycle Waste Heat Recovery (WHR) systems are promising solutions to reduce fuel consumption for trucks. Due to coupling between engine and WHR system, control of these complex systems is challenging. This study presents an integrated energy and emission management strategy for an Euro-VI Diesel engine with WHR system. This Integrated Powertrain Control (IPC) strategy optimizes the CO_2-NO_x trade-off by minimizing online the operational costs associated with fuel and AdBlue consumption. Contrary to other control studies, the proposed control strategy optimizes overall engine-after-treatment-WHR system performance and deals with emission constraints. From simulations, the potential of this IPC strategy is demonstrated over a World Harmonized Transient Cycle (WHTC) using a high-fidelity simulation model. These results are compared with a state-of-the-art baseline engine control strategy. By applying the IPC strategy, an additional 2.6% CO_2 reduction is achieved compare to the baseline strategy, while meeting the tailpipe NO_x emission limit. In addition, the proposed low-level WHR controller is shown to deal with the cold start challenges.*

Résumé — **Une stratégie intégrée de gestion des émissions et de l'énergie pour un moteur Diesel avec un système WHR (*Waste Heat Recovery*)** — Les systèmes WHR basés sur le cycle de Rankine sont des solutions prometteuses pour réduire la consommation de carburant pour les camions. En raison du couplage physique entre le moteur et le système WHR, l'asservissement de ces systèmes est particulièrement difficile. Cette étude présente une stratégie intégrée de gestion des émissions et de l'énergie pour un moteur Diesel EURO-VI avec un système WHR. Cette stratégie IPC (*Integrated Powertrain Control*) optimise le compromis entre CO_2 et NO_x en minimisant les coûts d'exploitation liés à la consommation de carburant et d'AdBlue. Contrairement à d'autres algorithmes d'asservissement, la stratégie proposée ici optimise les performances globales du système moteur – post-traitement des gaz d'échappement – WHR tout en respectant les contraintes d'émissions. À partir de simulations, le potentiel de cette stratégie IPC est montré sur un WHTC (*World Harmonized Transient Cycle*) en utilisant un modèle de simulation haute-fidélité. Ces résultats sont comparés à une stratégie d'asservissement de référence. En appliquant la stratégie IPC, une réduction supplémentaire de 2,6 % CO_2 est obtenue, tout en respectant la limite légale de NO_x. En plus, la loi de commande bas niveau pour le WHR arrive à gérer les problèmes de démarrage à froid.

NOMENCLATURE

DOC	Diesel Oxidation Catalyst
DPF	Diesel Particulate Filter
EGR	Exhaust Gas Recirculation
IPC	Integrated Powertrain Control
PM	Particule Matter
SCR	Selective Catalytic Reduction
VTG	Variable Turbine Geometry
WHR	Waste Heat Recovery
WHTC	Word Harmonized Transient Cycle

INTRODUCTION

With the implementation of Euro-VI emission legislation, tailpipe emissions are forced towards near zero impact levels. During the last two decades, nitrogen oxides (NO_x) and Particulate Matter (PM) emissions are reduced by 86% and 95%, respectively, for trucks. To meet these targets, a combination of engine measures (common rail fuel injection equipment, advanced turbocharging, Exhaust Gas Recirculation (EGR)) and aftertreatment systems (soot filters, catalysts) are applied.

As illustrated in Figure 1 [1], it has been increasingly challenging to keep the fuel consumption (and thus CO_2 emission) around the current level for each emission phase. However, driven by concerns about global warming and energy security, attention for heavy-duty applications currently also moves towards CO_2 emission reduction. On top of the current targets for pollutants, up to 20% CO_2 reduction has to be achieved in 2020 compared to the 2010 standards in the US [2]. Similar measures are discussed now in Europe [3].

For distribution trucks, garbage trucks and city buses, hybrid-electric drivetrains attract much attention to reduce CO_2 emissions. These drivetrains are less effective for long haul truck applications. In these cases, Waste Heat Recovery (WHR) seems a very promising technology [4-6]; in WHR systems, energy is recovered from heat flows, as illustrated in Figure 2 [7].

Up to 6% fuel consumption reduction has been demonstrated [4, 6]. However, control studies mainly focus on low level WHR system control [8-12]. Only a very few studies concentrate on energy management strategies for the complete engine [13]. However, these studies do not deal with the impact of the WHR system on emissions.

In this study, a cost-based optimization strategy is presented that explicitly deals with the requirements for CO_2 and pollutant emissions [7]. This strategy integrates energy and emission management and exploits the interaction between engine, aftertreatment and WHR system: Integrated Powertrain Control (IPC). Contrary to earlier work [14], a high fidelity WHR model is applied, which includes WHR dynamics and a low-level WHR controller. As a result, the simulation model combines a detailed aftertreatment and WHR system model and differs from the simplified control model that is embedded in the IPC strategy.

This work is organized as follows. First, the studied powertrain and applied simulation and control models are presented in Section 1. Section 2 discusses the

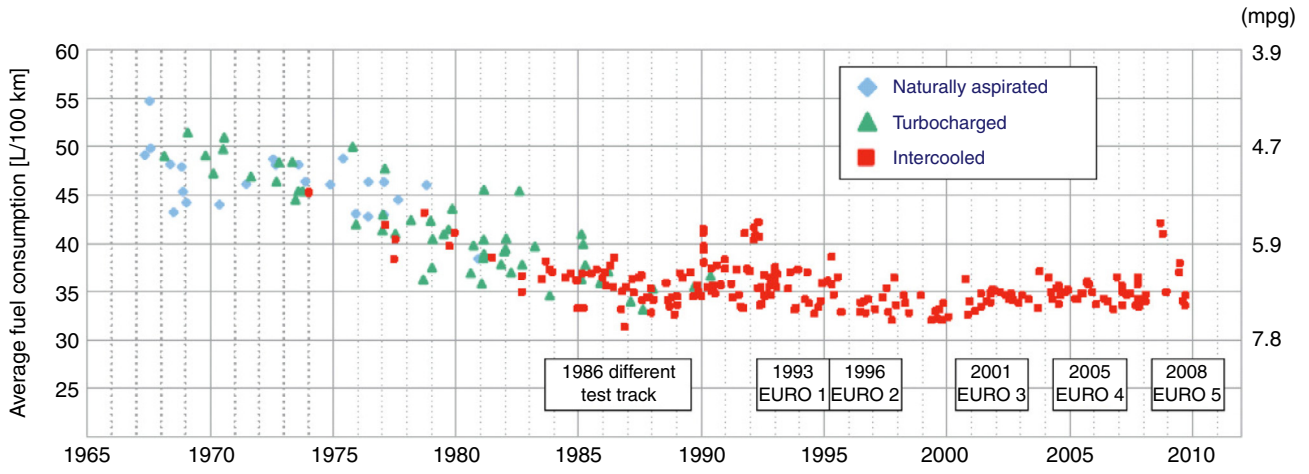

Figure 1

Historic fuel consumption for 40 ton trucks [1].

developed IPC strategy, whereas the control design is described in Section 3. For a World Harmonized Transient Cycle (WHTC), the results of this IPC strategy are compared with the results of a baseline engine control strategy in Section 4. Finally, conclusions are drawn and directions for future research are sketched.

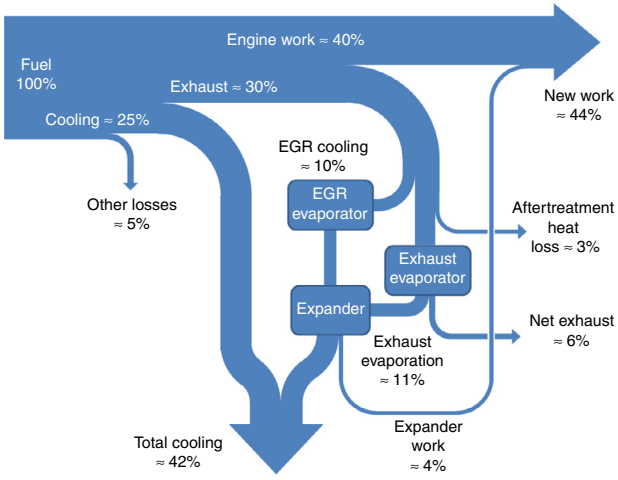

Figure 2

Sankey diagram of engine with WHR system [7].

1 SYSTEM DESCRIPTION

Figure 3 shows a scheme of the examined engine platform. It is based on a 6 cylinder, 13 liter, 375 kW Euro-VI Diesel engine, which is equipped with a cooled Exhaust Gas Recirculation (EGR) system and a turbocharger with Variable Turbine Geometry (VTG). Furthermore, an exhaust gas aftertreatment system is installed. This system consists of a Diesel Oxidation Catalyst (DOC), a Diesel Particulate Filter (DPF) and an urea-based Selective Catalytic Reduction (SCR) system.

The DPF system removes the particulates from the exhaust flow. To avoid clogging of the filter, fuel is periodically injected upstream of the DOC. As a result, the exhaust gas temperature is raised, such that the trapped particulates are oxidized. The remaining NO_x emissions downstream of the DPF system are converted into harmless products (nitrogen and water) over the 32.6 liter Cu-Zeolite SCR catalyst. For this catalytic process, ammonia (NH_3) is required. This is partly formed upstream of the catalyst by decomposition of the injected aqueous urea solution (trade name: AdBlue) in the hot exhaust gases. Further decomposition takes place in the SCR catalyst. To avoid unacceptable NH_3 slip, an ammonia oxidation catalyst (AMOX) is installed.

In this study, the Euro-VI engine is extended with a Waste Heat Recovery (WHR) system. This system is

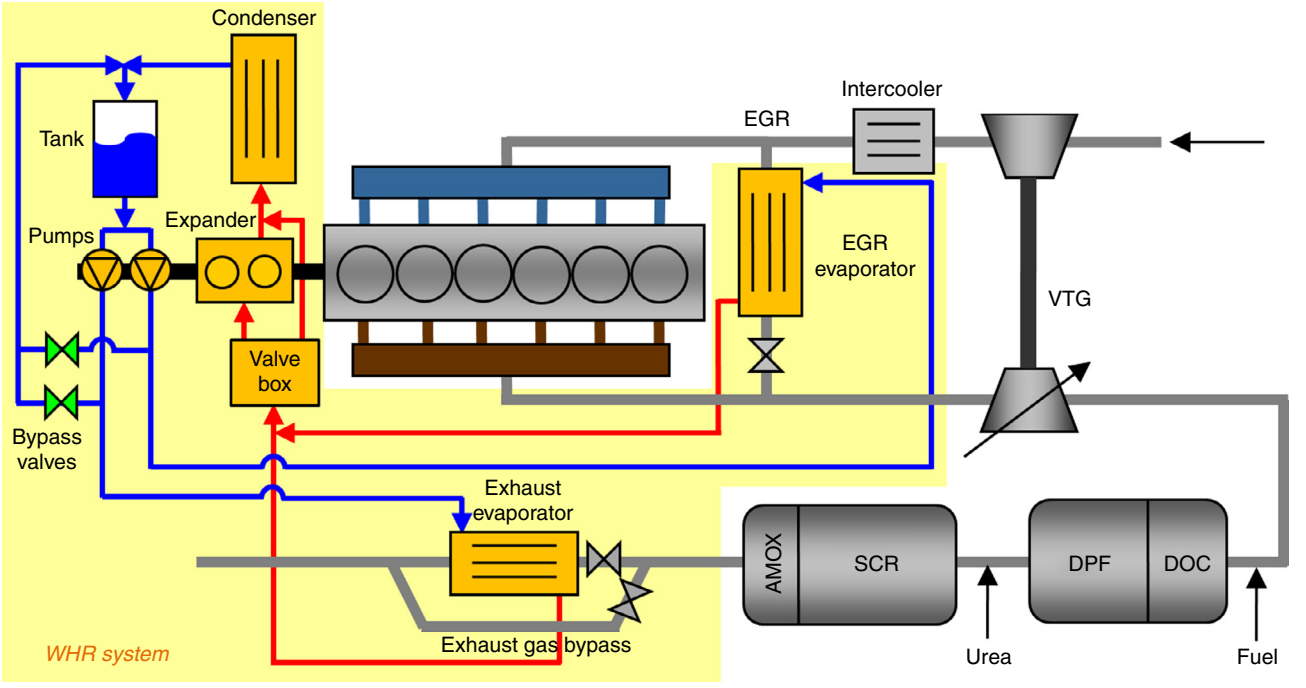

Figure 3

Scheme of the studied Euro-VI engine with WHR system [16].

based on a Rankine cycle, in which thermal energy is recovered from both the EGR line and exhaust line using two individual evaporators. The recovered exhaust heat is converted to mechanical power using a piston expander. The piston expander and pumps are mechanically coupled with the engine crankshaft. Consequently, the recovered power is directly transmitted to the engine. The working fluid mass flow through both evaporators is controlled by two bypass valves. As this is a closed system, the working fluid is cooled over the condenser, such that it is in liquid phase at the entrance of the pumps. It is noted that the heat input from the exhaust gas can be limited using the exhaust gas bypass. However, this operation mode is not considered in this study.

The following sections give a description of the applied simulation and control model.

1.1 Simulation Model

1.1.1 Engine

To describe the engine behavior, engine maps of the exhaust gas mass flow $\dot{m}_{exh}$, exhaust gas temperature T_{exh} and engine out NO_x mass flow $\dot{m}_{NO_x}$ are applied. These four-dimensional maps $f(N_e, \tau_e, u_{EGR}, u_{VTG})$ are constructed using a validated mean-value engine model. For varying combinations of EGR valve position u_{EGR} and VTG position u_{VTG}, the fuel mass flow $\dot{m}_f$ is varied such that the requested torque $\tau_{d,req} = \tau_e$ is realized (with constant engine speed N_e (rpm)). Note that these maps are determined for the engine without WHR system.

1.1.2 Aftertreatment System

A high fidelity aftertreatment model is implemented to simulate the DOC/DPF and SCR system. This modular model is built up using one-dimensional submodels of a pipe with urea decomposition, pre-oxidation catalyst (DOC), DPF, SCR catalyst, and ammonia oxidation (AMOX) catalyst. All catalyst models are based on first principle modeling and consist of mass and energy balances. By dividing the catalyst in various segments, these validated models describe the spatial distribution of pressure, temperature and chemical components. Further details on the model approach and SCR model can be found in [15].

1.1.3 Waste Heat Recovery System

For the description of the WHR system, we applied the model that is presented in [16]. This model is fitted and validated over a wide operating range. In this model, the pumps and expander are described by stationary maps, whereas the valves are described by stationary relations. The piping within the WHR system model are represented by volumes. These volumes are modeled as incompressible pressure volumes and compressible pressure volumes for the liquid case and vapor case, respectively.

As the main WHR system dynamics correspond to the evaporators, condenser and pressure volumes, the modeling of these components is briefly reviewed in the sequel of this section.

1.1.3.1 Evaporators and Condenser

The evaporators and condenser are counter flow type of heat exchangers. Their models can be separated in three parts: the working fluid, the heat exchanger wall and the secondary fluid. The working fluid is pure ethanol, while the secondary fluid is exhaust gas for the evaporator case and coolant for the condenser case. The model is given by a set of non-linear partial differential equations which describe the conservation of mass and energy.

Conservation of mass (working fluid):

$$V_{wf}\frac{\partial \rho_{wf}}{\partial t} + L\frac{\partial \dot{m}_{wf}}{\partial z} = 0 \tag{1}$$

Conservation of energy:

$$\rho_{wf}V_{wf}\frac{\partial h_{wf}}{\partial t} = -\dot{m}_{wf}L\frac{\partial h_{wf}}{\partial z} + \alpha_{wf}S_{wf}(T_w - T_{wf}) \tag{2a}$$

$$\rho_g V_g \frac{\partial h_g}{\partial t} = \dot{m}_g L\frac{\partial h_g}{\partial z} - \alpha_g S_g(T_g - T_w) \tag{2b}$$

Conservation of energy at the wall:

$$\rho_w V_w c_{pw}\frac{\partial T_w}{\partial t} = \alpha_g S_g(T_g - T_w) + \alpha_{wf}S_{wf}(T_{wf} - T_w) \tag{3}$$

where h_{wf} is the working fluid enthalpy, h_g is the exhaust gas enthalpy, $\dot{m}_{wf}$ and $\dot{m}_g$ are the mass flow rates of the working fluid and exhaust gas, respectively. The parameters used in the heat exchanger model are listed in Table 1. As a consequence of the evaporation process, the heat transfer coefficient on the working fluid side α_{wf} is characterized by three heat transfer coefficients: α_{wf}^{l} for liquid, α_{wf}^{tp} for two-phase and α_{wf}^{v} for vapor. To account for phase change, mathematical equations for the working fluid properties are derived using Figure 4.

The model given by Equations (1, 2) and (3) is discretized with respect to time and space based on a finite difference approximation. The resulting expressions are a set of difference dynamic equations, which are used to

TABLE 1
Heat exchanger and pressure volume model parameters

Symbol	Unit	Description
c_p	J/kg·K	Specific heat capacity at constant pressure
c_{pg}	J/kg·K	Exhaust gas specific heat capacity
c_{pw}	J/kg·K	Wall mass specific heat capacity
c_v	J/kg·K	Specific heat capacity at constant volume
L	m	Heat exchanger tube length
R	J/kg·K	Ideal gas constant
S_{wf}	m^2	Surface area of the working fluid
S_g	m^2	Surface area of the exhaust gas
V	m^3	Volume
V_g	m^3	Volume of the exhaust gas side
V_w	m^3	Wall volume
V_{wf}	m^3	Volume of the working fluid side
α_{wf}	$W/m^2·K$	Working fluid heat transfer coefficient
α_g	$W/m^2·K$	Exhaust gas heat transfer coefficient
ρ_{wf}	kg/m^3	Working fluid density
ρ_g	kg/m^3	Exhaust gas density
ρ_w	kg/m^3	Wall density

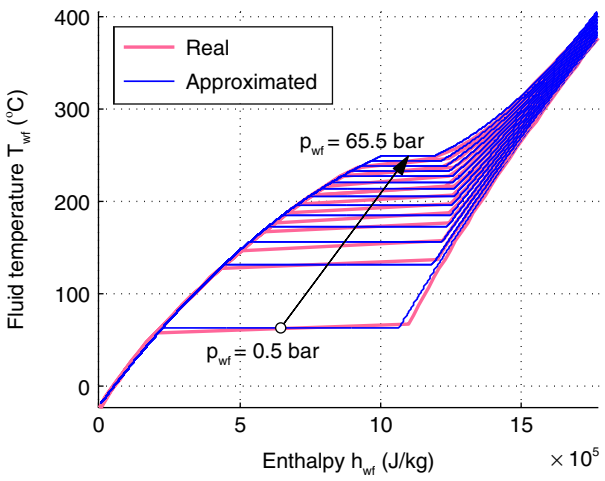

Figure 4

Ethanol temperature as a function of specific enthalpy and pressure [16].

compute the evaporator model output variables. These output variables are the outlet temperatures for the exhaust gas and working fluid side, respectively.

1.1.3.2 Pressure Volumes

The compressible pressure volume model assumes that the working fluid is in superheated vapor state and that it behaves like an ideal gas. Based on the laws for mass and energy conservation, the following equations are derived:

$$\frac{dm}{dt} = \dot{m}_{in} - \dot{m}_{out} \tag{4a}$$

$$m\frac{dT}{dt} = bT_{in} + aT \tag{4b}$$

$$mT\frac{dp}{dt} = (bT_{in} + aT)p + mT\frac{R}{V}(\dot{m}_{in} - \dot{m}_{out}) \tag{4c}$$

where a and b are defined as:

$$\begin{aligned} a &= -\dot{m}_{in} - \left(\frac{c_p}{c_v} - 1\right)\dot{m}_{out} \\ b &= \frac{c_p}{c_v}\dot{m}_{in} \end{aligned} \tag{5}$$

Note that these equations depend on both temperature and mass flow rates. For steady state conditions, Equations (4b, c) reduce to $T = -\frac{b}{a}T_{in} = T_{in}$, respectively.

1.2 Control Model

This section presents the control model that is embedded in the optimal control strategy in Section 2. For real-world implementation, this simplified model has to represent the main system characteristics and has to be evaluated in real-time. Compared to the simulation model, the main difference lies in the description of the aftertreatment and WHR system; identical engine maps are applied.

1.2.1 Waste Heat Recovery System

In contrast with [14], the actual net mechanical WHR power output $P_{WHR} = \tau_{WHR} \cdot \omega_{WHR}$ is assumed to be available in the supervisory controller. Consequently, no explicit WHR model description is used in the controller.

By assuming ideal torque management, the requested engine torque is determined from:

$$\tau_{e,req} = \tau_{d,req} - \tau_{WHR} \tag{6}$$

with the actual produced WHR torque τ_{WHR} (Nm) available from the simulation model.

1.2.2 Aftertreatment System

The thermal behavior of the total DOC-DPF-SCR system is described by two coupled differential equations, Equation (8). Note that the DOC-DPF system behavior is lumped in one equation. For the SCR conversion efficiency η_{SCR}, a set of three stationary maps is used, which are determined for different pre-SCR concentration ratios $C_{NO_2}/C_{NO_x} = (0, 0.5, 1.0)$ and for a specified ammonia slip level. From Figure 5, it is seen that the individual SCR efficiency map depends on the average SCR catalyst temperature T_{SCR} (°C) and space velocity SV (1/h):

$$SV = 3\,600 \cdot \frac{\dot{m}_{exh}}{\rho_{exh} V_{cat}} \tag{7}$$

with normal condition exhaust gas density $\rho_{exh}(\mathrm{g/m^3})$ and SCR catalyst volume $V_{cat}(\mathrm{m^3})$. Using the predicted C_{NO_2}/C_{NO_x} ratio from a stationary DOC efficiency map, the NO_x conversion efficiency is computed by interpolation.

In summary, the control model is written in state space form $\dot{x} = f(x)$:

$$\dot{x} = \begin{bmatrix} c_1 \cdot \dot{m}_{exh}(T_{exh} - T_{DOC}) \\ c_2 \cdot \dot{m}_{exh}(T_{DOC} - T_{SCR}) - c_3(T_{SCR} - T_{amb}) \\ \dot{m}_{NO_x}(1 - \eta_{SCR}(T_{SCR}, SV, C_{NO_2}/C_{NO_x})) \end{bmatrix} \tag{8}$$

with state variables:

$$x = \begin{bmatrix} T_{DOC} \\ T_{SCR} \\ m_{NO_x,tp} \end{bmatrix} = \begin{bmatrix} \text{DOC catalyst temperature} \\ \text{SCR catalyst temperature} \\ \text{Tailpipe } NO_x \text{ mass} \end{bmatrix}$$

The applied model parameters are specified in Table 2.

TABLE 2
Control model parameters

Constant	Unit	Definition	Value
c_1	$\mathrm{kg^{-1}}$	$\frac{c_{p,exh}}{C_{DOC}}$	0.1163
c_2	$\mathrm{kg^{-1}}$	$\frac{c_{p,exh}}{C_{SCR}}$	0.0512
c_3	$\mathrm{s{\cdot}kg^{-1}}$	$\frac{h}{C_{SCR}}$	1.0000

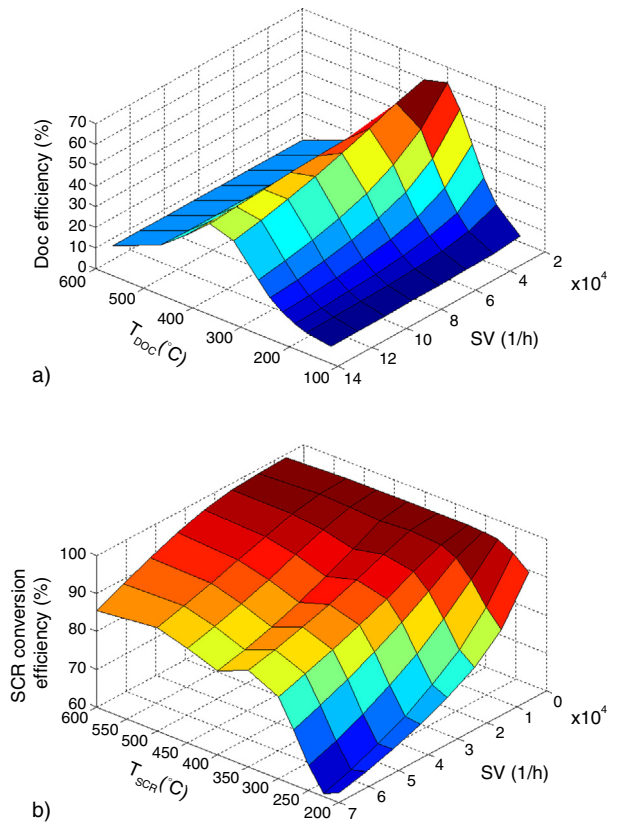

Figure 5

a) DOC efficiency map C_{NO_2}/C_{NO_x} and b) SCR efficiency map for $C_{NO_2}/C_{NO_x} = 0.5$.

2 CONTROL STRATEGY

The main goal of the engine control system is to determine the settings for the control inputs:

$$u^T = [\dot{m}_f \ \dot{m}_a \ u_{EGR} \ u_{VTG} \ u_{WHR,EGR} \ u_{WHR,exh}]$$

such that fuel consumption $\dot{m}_f$ is minimized within the constraints set by emission legislation. As illustrated in Figure 6, the available manipulated variables are the AdBlue dosing quantity $\dot{m}_a$, EGR valve position u_{EGR}, VTG rack position u_{VTG}, and WHR bypass valve position $u_{WHR,EGR}$ and $u_{WHR,exh}$.

To satisfy these requirements, the Integrated Powertrain Control (IPC) approach, which is introduced in [17], is followed. It is a model-based control design philosophy for combined engine-aftertreatment-energy recovery systems that:

- minimizes fuel consumption, while meeting emission constraints;
- offers a robust emission control solution for both test cycles and real-life operation;

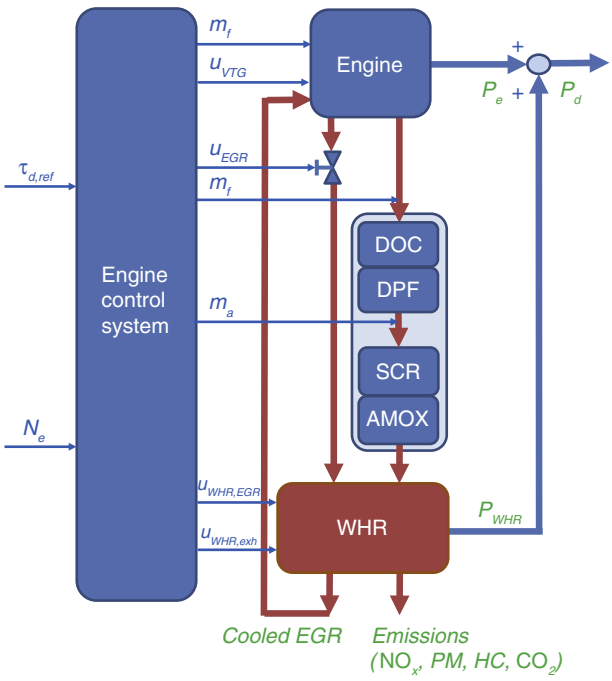

Figure 6

Overview of the engine control problem.

– deals with complex system interactions;
– uses models and optimal control theory to derive optimal control strategies;
– relaxes the calibration complexity.

In this systematic approach, the performance of the separate low-level controllers is coordinated by a supervisory controller, Figure 7. Based on information of the actual status and the driver's torque request, this controller determines the desired control settings using on-line optimization. With the available prediction of NO_x and PM reduction of the DPF-SCR system and WHR power output, the IPC strategy specifies the engine settings that give the required exhaust gas temperature, EGR and air flow, and engine out emissions to minimize operational costs (and thus fuel consumption) within the limits set for tailpipe emissions.

The developed IPC strategy is compared with a baseline engine control strategy, for reference. The examined control strategies are described below.

2.1 Optimization Problem

Following the IPC approach, the studied control problem is formulated in the optimal control framework. We propose to minimize the total operational costs associated with fuel, AdBlue consumption and active DPF regeneration. Consequently, the following objective function is defined:

$$\min_{u_d} \int_0^{t_e} w(N_e, \tau_d) \cdot \left[\pi_f \dot{m}_f + \pi_a \dot{m}_a + \pi_{PM} \dot{m}_{PM}\right] dt \qquad (9)$$

subject to:

$$\frac{\int_0^{t_e} \dot{m}_{\mathrm{NO}_{x,tp}}\, dt}{\int_0^{t_e} \frac{P_d}{3.6\times10^6}\, dt} \leq Z_{\mathrm{NO}x}\,(\text{tail} - \text{pipe NO}_x \text{ limit}) \qquad (10)$$

with Diesel price $\pi_f = 1.34 \times 10^{-3}$ Euro/g, AdBlue price $\pi_a = 0.50 \times 10^{-3}$ Euro/g, and fuel costs associated with active DPF regeneration per gram of accumulated soot $\pi_{PM} = 7.10 \times 10^{-2}$ Euro/g. In this case, the EGR valve position and VTG rack position are the selected decision variables: $u_d^T = [u_{EGR} u_{VTG}]$.

Assuming that all injected urea decomposes in ammonia and is available for NO_x conversion, the desired AdBlue dosage $\dot{m}_a$ (g/s) in Equation (9) is determined from:

$$\dot{m}_a = c_5 \cdot \eta_{SCR}(T_{SCR}, SV, C_{\mathrm{NO}_2}/C_{\mathrm{NO}_x}) \cdot \dot{m}_{\mathrm{NO}_x} \qquad (11)$$

where $c_5 = 2.0067$ and $\dot{m}_{\mathrm{NO}_x}$ (g/s) is the engine out NO_x emission. With the weighting function $w(N_e, \tau_d)$, it is aimed to capture the desired performance independent of the applied test cycle, see also Section 3.

2.2 IPC Strategy

For this optimization problem, Pontryagin's Minimum Principle is applied to find an optimal solution, see, *e.g.*, [18]. Accordingly, a Hamiltonian is formulated which entails the objective function from Equation (9) augmented with Lagrange multipliers λ and the state dynamics $f(x)$ from Equation (8):

$$H = w(N_e, \tau_d) \cdot \left[\pi_f \dot{m}_f + \pi_a \dot{m}_a + \pi_{PM} \dot{m}_{PM}\right] + \lambda^T f(x) \qquad (12)$$

These Lagrange multipliers represent equivalence price parameters and have the following interpretation:
– λ_1 represents a cost-equivalent parameter for a DOC/DPF temperature rise of 1°C within 1 s. A larger value will result in higher T_{DOC};
– λ_2 represents a cost-equivalent parameter for a SCR temperature rise of 1°C within 1 s. By increasing its value, a better heat transfer between DOC/DPF and SCR can be achieved, and so a better SCR conversion efficiency;
– λ_3 takes into account the accumulated tailpipe NO_x emissions. A higher value will more penalize the raw engine out NO_x emissions;

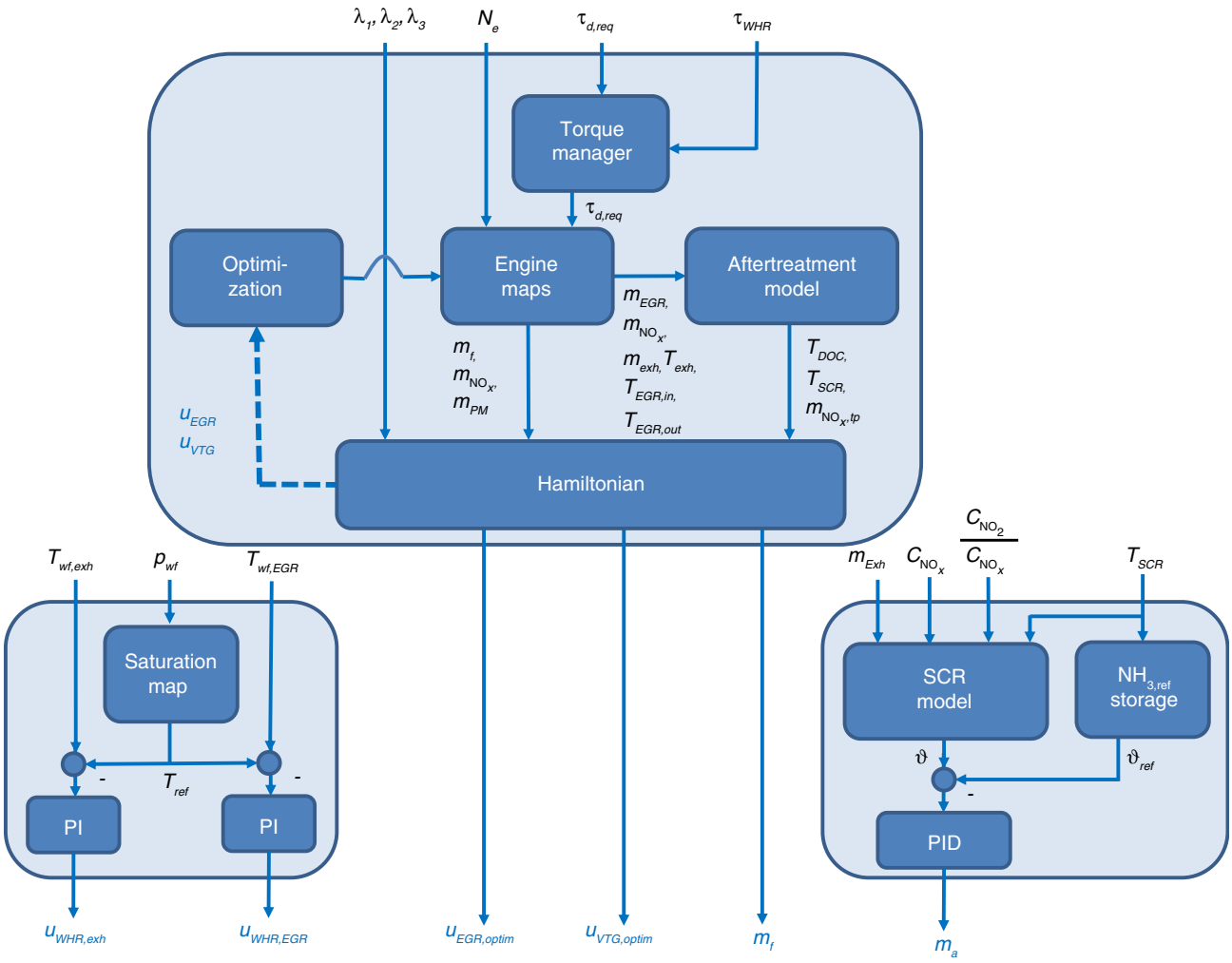

Figure 7

Scheme of the proposed engine control system.

Two necessary conditions for optimality of the solution u_d can be formulated:

$$-\frac{\partial H}{\partial x} = \dot{\lambda} \tag{13}$$

$$\frac{\partial H}{\partial u_d} = 0 \tag{14}$$

From these conditions, it is easily seen that λ_3 remains constant for the optimal solution, and only depends on its initial conditions $\lambda_3(0)$. More important, the dynamics of λ_1 and λ_2 are unstable and have end-point constraints. These two facts make the solution to this optimal control problem difficult to implement in practice, as it requires the entire drive cycle to be known *a priori*.

As we want to use the presented systematic framework, the pragmatic approach that is described in [19] is followed; the course of λ_1 and λ_2 are determined by a heuristic, postulated rule parameterized by λ_T, ΔT_1 and ΔT_2. This approach is illustrated in Figure 8. The effort to heat up the aftertreatment system is assumed to be proportional to the SCR inefficiency $1 - \eta_{SCR}$. When T_{DOC} is lower or marginally higher than T_{SCR}, it seems better to invest in raising the engine-out exhaust temperature rather than promoting heat convection from DOC/DPF to SCR (high λ_1). The converse holds when T_{DOC} T_{SCR} (high λ_2).

This sub-optimal controller is implemented in the presented simulation model. At every time step over the studied test cycle, the Hamiltonian, Equation (12), is

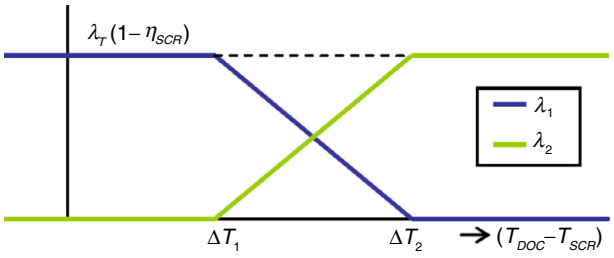

Figure 8
Heuristic rule for λ_1 and λ_2 [19].

numerically optimized on-line using a bounded 2D gradient descent method for the specified set of Lagrange multipliers λ. In Section 3, the off-line calibration of these multipliers is discussed.

2.3 Baseline Strategy

For the baseline engine control strategy, we mimic a state-of-the-art air management strategy for a standard Euro-VI engine configuration (without WHR system). This strategy is characterized by switching between two control modes:

- thermal management mode (M1) for rapid heat-up of the aftertreatment system ($T_{SCR} < 200°C$);
- low NO_x mode (M2) for normal operation ($T_{SCR} \geq 250°C$).

A fundamental difference with the IPC strategy is that the baseline strategy relies on fixed control settings (u_{EGR}, u_{VTG}) for each engine operating point (N_e, τ_e). For both modes, these settings are pre-determined in an off-line optimization procedure, which is often based on stationary test conditions.

As we want to use the same control structure for both strategies in simulations, two different sets of constant λ are used for the control modes (*Tab. 3*). The current engine calibration is mainly optimized using steady state measurements. Therefore, anticipated steady-state T_{DOC} and T_{SCR} values from the engine maps are used in the Hamiltonian to evaluate the SCR efficiency maps, instead of the momentary temperatures.

3 CONTROL DESIGN

This section discusses the control design procedure for the applied strategies. An overview of the selected control parameters is given in Table 3.

TABLE 3
Selected control parameters

Control strategy	Control parameters			
	$-\lambda_{(1,M1)}$	$\lambda_{(1,M2)}$	λ_2	λ_3
Baseline-(WHR)	2.0×10^{-5}	0	0	6.8×10^{-3}
Recal-WHR	1.2×10^{-5}	0	0	4.88×10^{-3}
	$-\lambda_T$	ΔT_1	ΔT_2	λ_3
IPC-WHR	1.6×10^{-5}	67.4	92.5	2.0×10^{-4}

TABLE 4
Emission targets for control design

Cycle	$NO_{x,eo}$ (g/kWh)	η_{SCR} (%)	Weight (%)	$NO_{x,tp}$ (g/kWh)
Cold WHTC	3.5	80	16	0.112
Hot WHTC	3.5	90	84	0.294
Weighted WHTC				0.406

3.1 Baseline Strategy with WHR System

For the baseline strategy, the control design boils down to the determination of:

- air management: engine maps for EGR valve and VTG settings by specifying the corresponding λ set for the control modes;
- SCR control: θ_{ref} map and PID-control settings;
- WHR control: PI-control settings.

These controllers have to be designed, such that the specified engineering target of 0.41 g/kWh is met. To realize this, a NO_x emission budget and averaged SCR conversion efficiencies η_{SCR} are specified for both cold and hot World Harmonized Transient Cycle (WHTC), Table 4.

3.1.1 Air Management

Following [19], two different sets of constant (λ_1, λ_3) are determined to specify the control modes of the baseline controller. For the low NO_x mode, $\lambda_{1,M2}$ and λ_2 are set to zero (no promotion of aftertreatment heat up), while λ_3 is tuned such that the engine out NO_x emission target

is reached over the WHTC. For the thermal mode, λ_3 is kept unchanged, whereas $\lambda_{1,M1}$ is tuned to get maximal T_{exh} increase within the targets set for engine out NO_x emission. This baseline Euro-VI case is the reference for the other studied strategies.

The baseline engine controller is also applied to the engine with WHR system (referred to as Baseline-WHR). In this case, the applied engine maps and controller settings are identical to the baseline strategy. However, the main difference is the implemented torque manager: the requested torque $\tau_{d,req}$ is realized by an ideal torque split, as described by Equation (6). This means that, compared to the baseline case, the engine will run in different operating points depending on the power delivered by the WHR system.

In the baseline-WHR case, the controller does not account for the effect of the WHR system on emissions. This can lead to relatively large deviations from the targets set for emissions. Consequently, this controller is tuned such that powertrain with WHR system is closely meeting the 0.41 g/kWh target again. This case is referred to as Recal-WHR and the corresponding new set (λ_1, λ_3) can be found in Table 3.

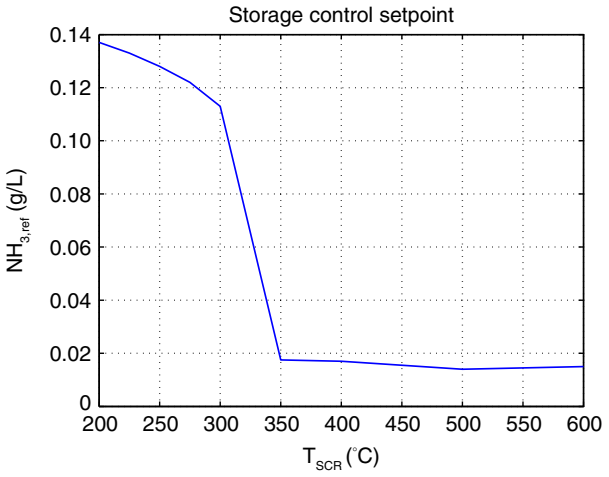

Figure 9

Reference ammonia storage θ_{ref}.

3.1.2 Low-Level SCR Control

For AdBlue dosing control, a model-based ammonia storage controller is applied. This low-level controller is based on a SCR catalyst model, which estimates the ammonia storage θ from SCR catalyst temperature T_{SCR} and pre-SCR NO_xemissions $\dot{m}_{NO_x}$ in real-time. This estimated value is compared with a reference value θ_{ref}. The difference is fed to the PID controller. By controlling θ, we aim to achieve high NO_x conversion efficiency and avoid excessive NH_3 slip in case of a sudden temperature increase. More details can be found in [20].

For the standard Euro-VI engine with baseline strategy, the static map $\theta_{ref}(T_{SCR})$ is calibrated, such that tailpipe NO_x emission meets the specified standards over the studied WHTC. Furthermore, cycle-averaged and peak tailpipe NH_3 emissions are kept within 10 and 25 ppm, respectively. The applied θ_{ref} map is shown in Figure 9. This SCR control calibration is used in all simulations.

3.1.3 Low-Level WHR Control

With the introduction of the high fidelity WHR system model, the two working fluid bypass valves $u_{WHR,exh}$ and $u_{WHR,EGR}$ have to be controlled. The main goal of this controller is to maximize power output P_{WHR}, within the constraints set by safe operation: the WHR system has to produce vapor in order to avoid damaging the expander. In this study, we focus on the power production mode; *e.g.*, start-up and shut down procedures are not considered. Nevertheless, results for the cold WHTC are also presented in Section 4.

Analogue to [12], two parallel PI controllers are implemented to control the post-EGR and post-exhaust evaporator temperature to their desired values (*Fig. 7*):

$$u_{WHR,i} = K_{P,i} \cdot (T_{ref} - T_{wf,i}) + K_{I,i} \int_0^{t_e} (T_{ref} - T_{wf,i}) dt \tag{15}$$

where $i = \{EGR, exh\}$ and T_{ref} is determined from the saturation vapor curve of the working fluid:

$$T_{ref}(p_{wf}) = T_{sat}(p_{wf}) + \Delta T_{sat} \tag{16}$$

with safety margin $\Delta T_{sat} = 10°C$.

As in [21], a PI controller with bumpless transfer mode and anti-windup method is implemented. In this study, the WHR control parameters $K_{P,i}$ and $K_{I,i}$ are manually tuned and chosen to be constant over the complete operating envelope, Table 5. For details on the low-level WHR control design, the reader is referred to [22].

3.2 IPC Strategy

For the IPC strategy, the following sets of control parameters have to be specified:

TABLE 5
Selected WHR control parameters

EGR bypass valve		Exhaust bypass valve	
$K_{P,EGR}$	–8	$K_{P,exh}$	–6
$K_{I,EGR}$	–7	$K_{I,exh}$	–6

– weighting function $w(N_e, \tau_d)$;
– Lagrange multipliers and their related variables: $\Delta T_1, \Delta T_2, \lambda_T$ and λ_3.

3.2.1 Weighting Function

Figure 10 shows the applied weighting function $w(N_e, \tau_d)$. For the studied cold and hot WHTC, typical operating points corresponding to high way driving are weighted more heavily, such that more attention is paid to minimize the operational costs during long haul driving conditions.

3.2.2 Lagrange Multipliers

To minimize the objective function over the studied cycle, a numerical minimization method is applied. This method aims to find the control parameters $\Delta T_1, \Delta T_2, \lambda_T$ and λ_3 that minimize the operational costs over the hot WHTC cycle, while the weighted tailpipe NO_x emissions stay within the specified limits. For this purpose, the cumulative cycle costs are evaluated. By applying the Nelder-Mead simplex method, the optimal set of control parameters is found that corresponds to the lowest costs over the studied duty cycle (*Tab. 3*).

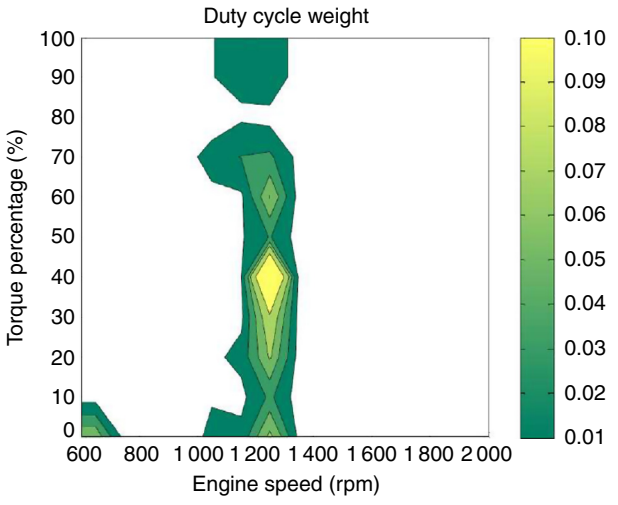

Figure 10
Weighting function $w(N_e, \tau_d)$ [19].

4 SIMULATION RESULTS

To evaluate the performance of the four proposed controllers in Table 3, simulations are done over the WHTC, which is shown in Figure 11. This cycle specifies the requested engine speed N_e and torque $\tau_{d,req}$. Three parts can be distinguished: urban driving conditions (0-900 s), rural driving conditions (900-1380 s), and highway driving conditions.

As we focus on Euro-VI emission targets, results are generated for both cold and hot cycle conditions. In case of a cold cycle, the initial temperatures of the aftertreatment components and WHR system are set to 20°C; engine heat up is not modeled yet. According to Euro-VI legislation, results for the cold and hot cycle are combined using weights of 16% and 84%, respectively, to provide the overall cycle-averaged WHTC result. Table 6 summarizes the results of the studied cases.

4.1 Overall Powertrain Results

4.1.1 CO_2-NO_x Trade-off

Figure 12 shows the trade-off between the cycle-averaged CO_2 and NO_x emissions. The baseline case, representing a conventional Euro VI engine without WHR system, is used as reference. Results from the other cases are expressed as a percentage of the baseline case. The figure shows that simply adding a WHR system (Baseline-WHR) reduces CO_2 emission with 2.6% and tailpipe NO_x emission with 2.8%. Recalibrating the controller to exploit the tailpipe NO_x margin created by the WHR system (Recal-WHR) yields an extra 0.8% of CO_2 emission reduction (*Tab. 6*).

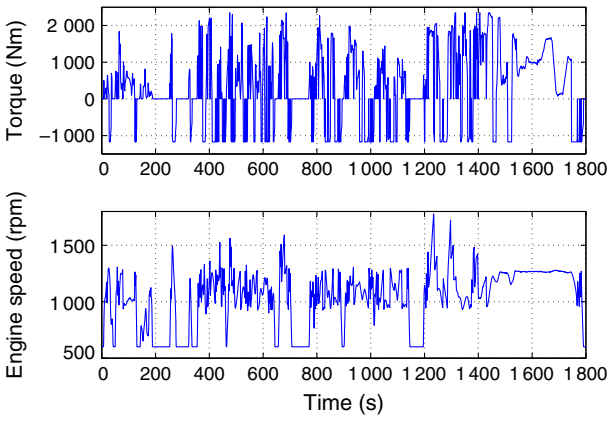

Figure 11
World harmonized transient cycle.

TABLE 6
Overview of WHTC results

Quantity	Control strategy			
	Baseline	Baseline -WHR	Recal -WHR	IPC -WHR
$NO_{x,eo}$ (g/kWh)				
Hot	3.45	3.32	3.38	5.08
Cold	3.61	3.49	3.57	5.06
Weighted	3.48	3.35	3.41	5.08
$NO_{x,tp}$ (g/kWh)				
Hot	0.348	0.338	0.356	0.369
Cold	0.730	0.716	0.689	0.616
Weighted	0.410	0.398	0.410	0.409
$NH_{3,max}$ (ppm)				
Hot	3	3	3	2
Cold	3	3	3	2
CO_2 (%)				
Hot	100	97.3	96.6	94.0
Cold	100	97.6	96.7	93.8
Weighted	100	97.4	96.6	94.0
WHTC Costs (%)				
Fuel	97.2	94.6	93.9	91.3
AdBlue	1.0	1.0	1.0	1.6
PM	1.8	1.8	1.7	1.0
Total	100	97.4	96.6	93.9

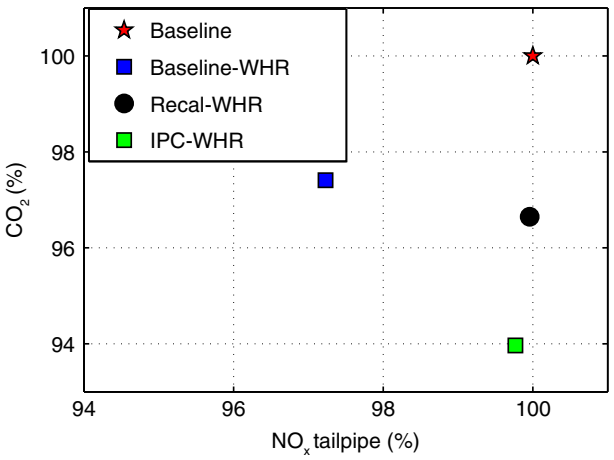

Figure 12
CO_2-NO_x trade-off for WHTC.

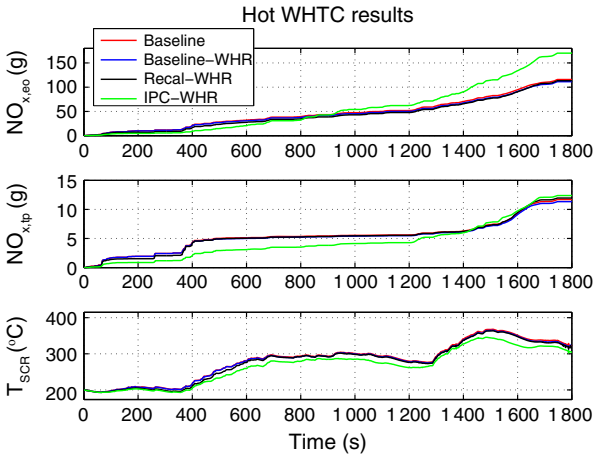

Figure 13
Cumulative emission results and SCR temperature (hot WHTC).

By implementing the IPC strategy on the powertrain equipped with WHR system, a further 2.6% reduction of CO_2 emission is achieved compared to the Recal-WHR case, without increasing tailpipe NO_x emission. This sums up to a total CO_2 reduction of 6% compared to the baseline strategy.

4.1.2 EGR-SCR Balancing

The IPC strategy is able to achieve the additional CO_2 reduction by determining on-line the cost-optimal balance between engine-out NO_x emission and SCR conversion efficiency at every time step: EGR-SCR balancing. From Figure 13, it is seen that the SCR temperature (and conversion efficiency) is relatively low at the start of the WHTC (0-400 s). During this period, the IPC strategy keeps the tailpipe NO_x emission low by applying more EGR and does not promote SCR heat-up, unlike the baseline strategies. Consequently, engine out NO_x emission is significantly lower compared to the baseline strategies. When the SCR temperature increased to a level where NO_x conversion is sufficiently high, the IPC strategy minimizes EGR, such that operational costs are minimized within the emission constraint.

Figure 14 shows the corresponding fuel and AdBlue consumption as well as the resulting operational costs over time. These results are given relative to the baseline. At every time instant t_k, the relative fuel consumption is determined by:

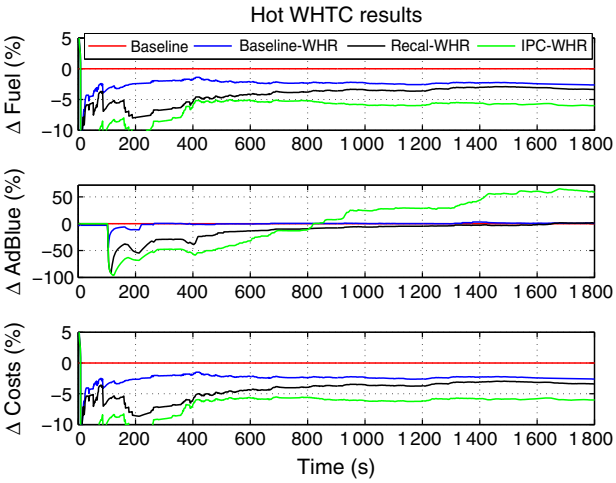

Figure 14

Operational costs and corresponding fuel and AdBlue consumption (hot WHTC). All results relative to the baseline.

$$\Delta Fuel(t_k) = 100 \cdot \frac{\int_0^{t_k} (\dot{m}_f - \dot{m}_{f,Baseline})dt}{\int_0^{t_k} \dot{m}_{f,Baseline}dt} \qquad (17)$$

In a similar way, the relative AdBlue and total operational costs are computed.

In the hot WHTC, the WHR system is active from the onset of the cycle. Due to the typical low load (and thus low waste heat) of the urban part of the WHTC, the WHR output is initially low, Figure 14. At $t = 400$ s, the WHR system alone (Baseline-WHR) has managed to save 1.5% of fuel and operational costs, while the Recal-WHR and IPC-WHR case have both saved around 5%. After this moment, the SCR system is heated up sufficiently; the IPC strategy starts to reduce the amount of EGR in order to reduce fuel consumption. This is done at the cost of increased engine-out NO_x emission and AdBlue consumption.

Over the entire hot WHTC, the IPC strategy managed to save around 6% of fuel, although the AdBlue consumption increased with over 50%. Due to the relatively low AdBlue consumption and costs in combination with reduced DPF regeneration costs, the total operational costs are reduced compared to the baseline strategies. More details on the operational costs can be found in Table 6.

4.1.3 WHR Effect

Figure 15 illustrates the WHR effect on powertrain performance for the hot WHTC. In the upper graph, the ratio of engine power (without WHR) P_e and requested power P_d is shown. It is observed that the WHR contribution is negligible during most of the rural part of the WHTC and during large idling periods (*Fig. 11*). Momentary, the WHR contribution shoots up to 100%. This occurs when the desired power P_d is very small, such that the WHR system fully produces the desired power. Note that some fuel will still be burnt in the diesel engine, since it still has to overcome (most of) its friction. It is not motoring during these periods as the desired power is still positive. Most WHR power is produced during the highway part of the WHTC, because the supply of waste heat to the evaporators is relatively high and constant. Recall that the IPC strategy is applying less EGR at the highway part, so it actually produces less WHR power compared to the other control strategies.

The two lower graphs of Figure 15 show the engine efficiency and the total powertrain efficiency, respectively:

$$\eta_{e,avg}(t_k) = \frac{\int_0^{t_k} P_e dt}{\int_0^{t_k} P_{fuel} dt}$$

$$\eta_{total,avg}(t_k) = \frac{\int_0^{t_k} (P_e + P_{WHR})dt}{\int_0^{t_k} P_{fuel} dt}$$

with $P_{fuel} = \dot{m}_f \cdot Q_{LHV}$ and the lower heating value Q_{LHV} of Diesel. In these graphs, the moving average of the efficiency is shown relative to the baseline:

$$\Delta\eta_{e,avg}(t_k) = \eta_{e,avg}(t_k) - \eta_{e,avg,Baseline}(t_k) \qquad (18)$$

$$\Delta\eta_{total,avg}(t_k) = \eta_{total,avg}(t_k) - \eta_{total,avg,Baseline}(t_k) \qquad (19)$$

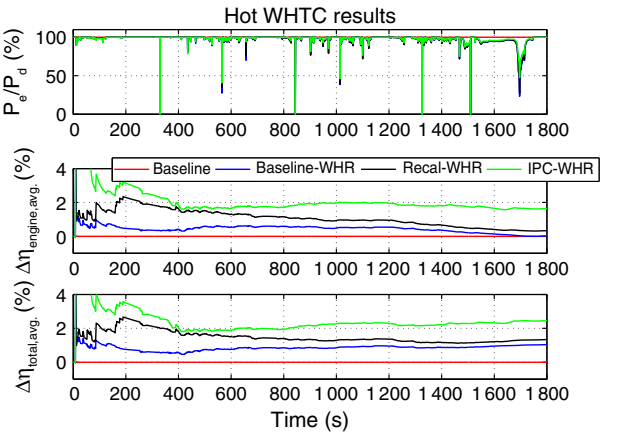

Figure 15

WHR effect on power output and efficiency (hot WHTC).

It is concluded that the IPC strategy is able to achieve a significant improvement in engine efficiency compared to the other strategies. This is the result of EGR-SCR balancing; due to different EGR valve and VTG rack settings, engine efficiency is increased. Comparison of $\eta_{e,avg}$ and $\eta_{total,avg}$ shows that the WHR system only has limited contribution for the IPC case. The Baseline-WHR and Recal-WHR strategies gain most in total efficiency due to the WHR system.

4.2 Low-Level WHR Controller

For the hot WHTC, the functionality of the low-level WHR controllers is illustrated in Figure 16. Based on the difference between $T_{ref}(p_{wf})$ and the actual post-evaporator temperature $T_{wf,i}$, the corresponding bypass valves are controlled. Recall from Equation (16) that the working fluid is in vapor phase, when $T_{wf,i} - T_{ref}(p_{wf}) > -\Delta T_{sat}$. From the two upper graphs, it is seen that both PI controllers are effective over the entire engine operating envelope; $T_{ref}(p_{wf})$ is tracked with a maximum absolute error of 10°C . The exhaust evaporator generates vapor over the entire hot WHTC. However, two phase flow is encountered downstream of the EGR evaporator around $t = 750$-800 s, despite the efforts of the PI controller: the EGR bypass valve is fully opened ($u_{WHR,EGR} = 0\%$). This is due to the low heat input during the preceding engine idling phase.

In general, the heat input during the urban part of the WHTC is relatively low. In this part, the working fluid flow through the evaporators is minimized by fully opening the EGR and exhaust bypass valves. As a result, the WHR power output P_{WHR} is small (*Fig. 15*). With increasing heat input in the rural and high way part, both bypass valves are gradually closed, especially the exhaust bypass $u_{WHR,exh}$. This leads to an increasing WHR power output: up to 7 kW for the IPC-WHR case. Note that $u_{WHR,EGR}$ is more closed in the baseline-WHR and recal-WHR cases towards the end of the WHTC. In this case, the IPC strategy reduces the EGR mass flow. To keep the working fluid in vapor phase, the controller responds by further opening the bypass valve, such that the EGR evaporator flow is reduced.

4.3 Cold Start WHTC Results

For the cold WHTC, the WHR system first has to heat up the working fluid to a superheated state before it can start to generate power. Although the current low-level WHR controller is not optimized for cold starts, the way it deals with cold starts is more than acceptable.

As shown in Figure 17, the EGR evaporator heats up significantly faster than the exhaust WHR evaporator. This is because the EGR evaporator is exposed to almost instant high temperatures, whereas the exhaust evaporator has to wait for the upstream aftertreatment system to heat up first. The ethanol inside the evaporators starts at 20°C for the cold start. This implies that the initial tracking error of the low level controller is around 70°C.

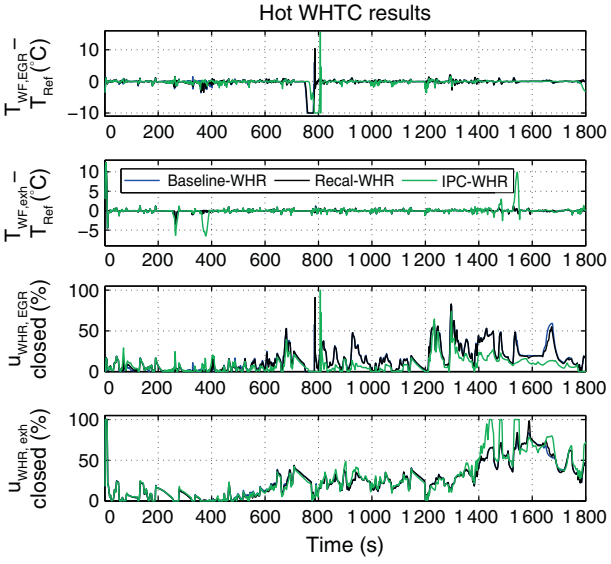

Figure 16

Operation of both PI WHR controllers during hot WHTC.

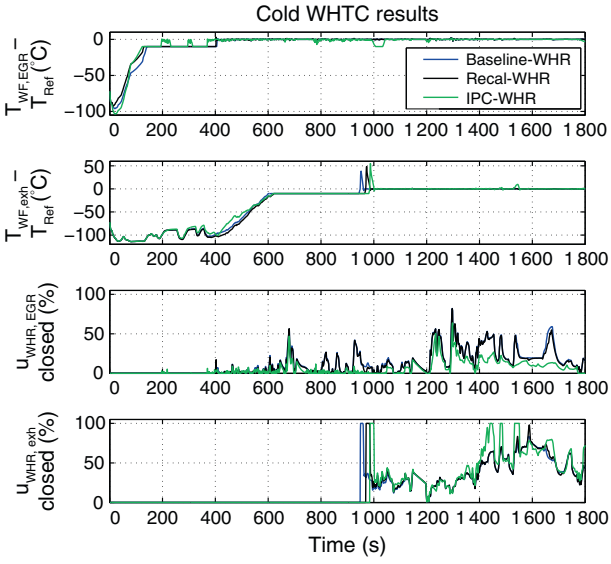

Figure 17

Operation of both PI WHR controllers during cold WHTC.

During heat-up, the low-level WHR controller keeps the bypass valves fully opened, such that a minimum amount of ethanol reaches the evaporators. The temperature of the ethanol in the evaporators rises until the saturation temperature is reached and evaporation starts. After evaporation is complete, the ethanol temperature quickly reaches its setpoint value. Then, the low-level WHR controller starts to close the working fluid bypass valves to increase the flow of ethanol to the evaporators. The second graph of Figure 17 shows that for the exhaust evaporator overshoot occurs at the end of the evaporation phase. Anti-windup is applied in the low-level WHR controllers to prevent excessive overshoot after the end of the evaporation phase. This same graph also shows that the tracking error can increase if the bypass valve saturates: $u_{WHR,exh} = 100\%$ (between 1 400 and 1 600 s).

CONCLUSIONS AND FUTURE WORK

A supervisory controller is presented for an Euro-VI engine with Waste Heat Recovery (WHR) system. This controller is rooted in the IPC approach and integrates energy and emission management. From simulation results over a WHTC, it is concluded that a recalibration of the baseline engine controller is required to use the full CO_2 reduction potential of the WHR system. With the IPC strategy, a systematic approach is introduced, which optimizes the CO_2-NO_x trade-off: additional 2.6% CO_2 reduction compared to the recalibrated baseline strategy (Recal-WHR).

Current research is dedicated to further development of the low-level WHR controller. Furthermore, tests will be performed on an engine dynamometer to demonstrate the potential of the proposed controllers. For the IPC strategy, focus is on the robustness for different duty cycles and on total energy management, which also includes the impact of the WHR system on the cooling system.

REFERENCES

1 ACEA (2011) *Commercial vehicles and CO_2* Report, ACEA.

2 EPA (2011) *EPA and NHTSA adopt first-ever program to reduce greenhouse gas emissions and improve fuel efficiency of medium-and heavy-duty vehicles*. Regulatory Announcement, August.

3 ACEA (2008) Vision 20-20. www.acea.be, September, ACEA Press Conference at the *IAA 2008*, Hanover, Germany.

4 Bredel E., Nickl J., Bartosch S. (2011) Waste heat recovery in drive systems of today and tomorrow, *MTZ Worldwide* **72**, 52-56.

5 Nelson C. (2009) Exhaust energy recovery, *Directions in Engine-Efficiency and Emissions, Research (DEER) Conference*, Dearborn, Michigan, 3-6 Aug.

6 Park T., Teng H., Hunter G.L., van der Velde B., Klaver J. (2011) A Rankine cycle system for recovering waste heat from HD Diesel engines - Experimental results, *SAE Paper* 2011-01-1337.

7 Kupper F. (2012) Integrated Powertrain Control for an Euro-VI heavy-duty Diesel engine with Waste Heat Recovery system, *Master's Thesis*, Eindhoven University of Technology.

8 Abbe Horst T., Rottengruber H.-S., Seifert M., Ringler J. (2013) Dynamic heat exchanger model for performance prediction and control system design of automotive waste heat recovery systems, *Applied Energy* **105**, 293-303.

9 Hou G., Sun R., Hu G., Zhang J. (2011) Supervisory predictive control of evaporator in Organic Rankine Cycle (ORC) system for waste heat recovery, *2011 International Conference on Advanced Mechatronic Systems*, Zhengzhou, China, 11-13 Aug., pp. 306-311.

10 Howell T., Gibble J., Tun C. (2011) Development of an ORC system to improve HD truck fuel efficiency, *Directions in Engine-Efficiency and Emissions, Research (DEER) Conference*, Detroit, Michigen, 3-6 Oct.

11 Quoilin S., Aumann R., Grill A., Schuster A., Lemort V., Spliethoff H. (2011) Dynamic modeling and optimal control strategy of waste heat recovery organic Rankine cycles, *J. Applied Energy* **88**, 6, 2183-2190.

12 Tona P., Peralez J., Sciarretta A. (2012) Supervision and control prototyping for an engine exhaust gas heat recovery system based on a steam Rankine cycle, *2012 IEEE/ASME International Conference on Advanced Intelligent Mechatronics*, Kaohsiung, Taiwan, 11-14 July, pp. 695-701.

13 Hounsham S., Stobart R., Cooke A., Childs P. (2008) Energy recovery systems for engines, *SAE Paper* 2008-01-0309.

14 Willems F., Kupper F., Cloudt R. (2012) Integrated energy & emission management for heavy-duty Diesel engines with waste heat recovery system, Proceedings of the *2012 IFAC Workshop on Engine and Powertrain Control, Simulation and Modeling (ECOSM'12)*, Rueil-Malmaison, France, 23-25 Oct., pp. 203-210.

15 Cloudt R., Saenen J., van den Eijnden E., Rojer C. (2010) Virtual exhaust line for model-based Diesel aftertreatment development, *SAE Paper* 2010-01-0888.

16 Feru E., Kupper F., Rojer C., Seykens X., Scappin F., Willems F., Smits J., de Jager B., Steinbuch M. (2013) Experimental validation of a dynamic waste heat recovery system model for control purposes, *SAE Paper* 2013-01-1647.

17 Willems F., Foster D. (2009) Integrated Powertrain Control to meet future CO_2 and Euro-6 emission targets for a Diesel hybrid with SCR-deNOx system, *IEEE Proc. of 2009 American Control Conference, St. Louis, MO, USA,* 10-12 June, pp. 3944-3949.

18 Geering H. (2007) *Optimal control with engineering applications*, Springer Verlag.

19 Cloudt R., Willems F. (2011) Integrated Emission Management strategy for cost-optimal engine-aftertreatment operation, *SAE International Journal of Engines* **4**, 1, 1784-1797.

20 Willems F., Cloudt R. (2011) Experimental demonstration of a new model-based SCR control strategy for cleaner heavy-duty diesel engines, *IEEE Transactions on Control Systems Technology* **19**, 5, 1305-1313.

21 Pramudya Indrajuana A. (2012) Control development for Waste Heat Recovery system on heavy duty trucks, *Master's Thesis*, Delft University of Technology.

22 Rascanu G. (2013) Integrated Powertrain Control for truck engines with Waste Heat Recovery system, *Master's Thesis*, Eindhoven University of Technology.

Manuscript accepted in November 2013
Published online in April 2014

Cite this article as: F. Willems, F. Kupper, G. Rascanu and E. Feru (2015). Integrated Energy and Emission Management for Diesel Engines with Waste Heat Recovery Using Dynamic Models, *Oil Gas Sci. Technol* **70**, 1, 143-158.